Molecular stabilization and angular distribution in photodissociation of H_2^+ in intense laser fields

Eric E. Aubanel, Jean-Marc Gauthier, and André D. Bandrauk
Laboratoire de Chimie Théorique, Faculté des Sciences, Université de Sherbrooke, Sherbrooke, Quebec, Canada J1K 2R1
(Received 12 November 1992)

Photodissociation probabilities of the H_2^+ molecule calculated from numerical solutions of the time-dependent Schrödinger equation exhibit minima for high-intensity ($10^{12} < I < 10^{14}$ W/cm^2) subpicosecond (100 fs) laser-pulse excitation. These minima are shown to correspond to stabilization of the molecular ion and hence to suppression of the photodissociation by the creation of stable laser-induced resonances by a laser-induced avoided-crossing mechanism between the field-molecule potentials. Rotational excitations are shown to destroy such stabilization at intensities above 10^{13} W/cm^2. Angular distributions of the photofragments demonstrate gradual molecular alignment with increasing intensity. Bimodal distributions can also occur and they are the signature of the stabilization mechanism.

PACS number(s): 33.90.+h, 33.80.Gj

I. INTRODUCTION

Atomic and molecular radiative interactions at high laser intensities such that Rabi frequencies approach electronic frequencies lead to new nonlinear, nonperturbative, physical phenomena such as above-threshold ionization (ATI) and very high harmonic generation [1,2]. Since high intensities are achieved only with short (very often subpicosecond) pulses, then coherent nonperturbative superpositions of quantum states are readily obtained. Both the nonperturbative and the coherent nature of such intense-laser excitations leads to prediction of stabilization, i.e., suppressions of ionization in atoms [3–7].

Similar phenomena can also occur in molecular multiphoton excitations [2,8]. In the present paper, we will focus on intensities between 10^{12} and 10^{14} W/cm^2 for which electronic Rabi frequencies approach or exceed molecular vibrational frequencies. In such cases, a useful concept derived from a dressed-state representation of field-matter interactions [1,9], is that of laser-induced avoided crossings [10–16]. Thus, as illustrated in Fig. 1 for the photodissociation of H_2^+, the initial ground-state field-molecule potential $W_1 = V_g(^2\Sigma_g^+) + n\hbar\omega$ crosses the dissociative $W_2 = V_u(^2\Sigma_u^+) + (n-1)\hbar\omega$ potential as a consequence of conservation of total energy after absorption of one photon. The radiative interaction or electronic Rabi frequency ω_R, for a field $E(t) = E_0\cos(\omega t)$, which can be written as

$$V_{gu}(R) = \langle {}^2\Sigma_u^+, n-1 | \mathbf{d}(R)\cdot\mathbf{E}_0/2 | {}^2\Sigma_g^+, n \rangle = \hbar\omega_R/2 , \quad (1)$$

$$\hbar\omega_R/2(\mathrm{cm}^{-1}) = 5.85\times10^{-4}[I(\mathrm{W/cm}^2)]^{1/2} d(\mathrm{a.u.}) = \gamma d , \quad (2)$$

is operative between the two states V_g and V_u, where $d(R)$ is the electronic dipole moment in atomic units (a.u.) and $\gamma = 5.85\times10^{-4}[I(\mathrm{W/cm}^2)]^{1/2}$/a.u. is a unit-conversion factor. Figure 1 shows that one can describe the molecular states either in the original unperturbed (crossing) state representation which we call *diabatic* states (dashed lines, Fig. 1). New field-induced states are obtained by diagonalizing the diabatic potential matrix

$$W(R) = \begin{bmatrix} V_g(R)+\hbar\omega & V_{gu}(R) \\ V_{gu}(R) & V_u(R) \end{bmatrix} . \quad (3)$$

This gives rise to laser-induced *adiabatic* molecular potentials

$$W_\pm(R) = \frac{V_g(R)+\hbar\omega+V_u(R)}{2} \pm \tfrac{1}{2}\{[V_g(R)+\hbar\omega-V_u(R)]^2+4V_{gu}(R)^2\}^{1/2} . \quad (4)$$

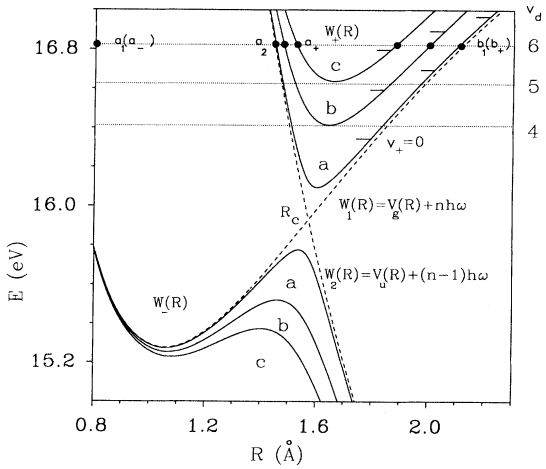

FIG. 1. Adiabatic W_+, W_- (solid lines) and diabatic W_1, W_2 (dashed lines) potentials for $\lambda = 212.8$ nm at I(W/cm^2): curve *a*, 3.2×10^{12}; curve *b*, 2.6×10^{13}; curve *c*, 5.2×10^{13}. Also shown are diabatic levels, $v_d = 4$, 5, 6 (dotted lines), adiabatic levels (horizontal bars), and turning points of W_1 (a_1,b_1), W_2 (a_2), W_+ (a_+,b_+), and W_- (a_-) at the energy of $v_d = 6$.

The upper potential (solid lines, Fig. 1) $W_+(R)$ will support new nuclear bound states $\chi_+(R)$ called *adiabatic* states or levels. These states are quasibound, i.e., they have a finite lifetime or energy width since in the new adiabatic representation, both bound $\chi_+(R)$ and continuum (dissociative) $\chi_-(R)$ states of the adiabatic potentials $W_\pm(R)$ remain coupled through the nonadiabatic interaction $-(\hbar^2/2m)\langle\psi_-(R)|d/dR|\psi_+(R)\rangle d/dR$, where $\psi_\pm(R)$ are the laser-induced adiabatic electronic functions [16,17]. A theory of the widths of these laser-induced quasidegenerate states as a function of molecular parameters was presented by Bandrauk and co-workers [14–16] in the dressed-state representation.

Figure 1 is based on the rotating-wave approximation (RWA), i.e., only resonant transitions are considered. In general since $E(t)=(E_0/2)(e^{i\omega t}+e^{-i\omega t})$, the first term induces the resonant transitions, whereas the $e^{-i\omega t}$ term will induce nonresonant, virtual, transitions. At higher intensities such that the electronic Rabi frequency ω_R, Eqs. (1) and (2), approach the excitation energy, RWA and Fig. 1 are no longer sufficient, i.e., more dressed states must be added [18–20]. Furthermore, in order to achieve high intensities, short pulses must be used. A dressed-state representation which depends on a slowly varying envelope approximation may no longer be adequate. For such a case a full time-dependent treatment will allow one to cover both limits, i.e., from the slowly varying envelope limit or dressed-state representation to the rapidly varying envelope case [21,22]. The latter case has recently been shown to produce important deviations from the dressed-state picture as a result of nonadiabatic transitions induced by the pulse variation itself [22].

In the present paper we shall focus on the photodissociation of H_2^+ and HD^+ to illustrate by time-dependent solutions of the Schrödinger equation the phenomenon of molecular *stabilization* or suppression of dissociation at high intensities through the mechanism of *laser-induced avoided crossings* illustrated in Fig. 1. Such stabilization was predicted by Bandrauk and co-workers [14–16] from the time-independent dressed-state representation, using the analogy between photodissociation and predissociation [23]. Recent experiments on intense-field photoionization of H_2 have interpreted anomalies in ATI spectra and proton-kinetic-energy distributions as due to the laser-induced crossing mechanism [24–29].

In our earlier time-independent or dressed-state work we have established the general rule of stabilization of laser-induced molecular states as a result of crossings (quasidegeneracies) of diabatic and adiabatic levels at critical field intensities [14–16]. Recent time-dependent calculations on the H_2^+ system illustrated in Fig. 1 have confirmed that stabilization can also occur in photodissociation induced by short pulses [22,30–32]. In the present paper, we examine in detail the correlation between the dressed-state interpretation of stabilization based on a coupled-equation approach and the exact time-dependent results based on solutions of the time-dependent Schrödinger equation. We also examine the effect of rotational excitations by presenting the photodissociation angular distributions of H_2^+ in the presence of short (100 fs) laser pulses at various intensities.

II. SEMICLASSICAL THEORY OF LASER-INDUCED RESONANCES

The additional nuclear degree of freedom, R, in H_2^+ as compared to atoms leads to the phenomenon of laser-induced avoided crossings. Such molecular laser-induced avoided crossings offer the possibility of creating laser-induced molecular quasibound states (see Fig. 1) or resonances for which a semiclassical stability analysis has been performed by Bandrauk and co-workers [14–16] in analogy to the semiclassical theory of molecular predissociation [23,33]. We summarize here the Fermi golden-rule weak-field regime and the strong-field adiabatic limit of radiative interaction.

The *diabatic* photodissociation width for weak radiative coupling V_{gu}, Eq. (2), is given by the standard perturbation Fermi golden-rule formula [23,33,34],

$$\Gamma_{v_d}(\mathrm{cm}^{-1})=2\pi\gamma^2\left|\int_0^\infty \chi_v(R)d(R)\chi_c(R)dR\right|^2 , \tag{5}$$

where γ is a unit-conversion factor defined in Eq. (2), $d(R)$ is the electronic transition moment in a.u., $\chi_v(R)$ is an initial bound-state vibrational function, and $\chi_c(R)$ is a final dissociative nuclear function, all parametrically dependent on the internuclear distance R. We now replace these functions by semiclassical (WKB) functions, i.e.,

$$\chi(R)=C[k(R)]^{-1/2}\sin[\phi(R)+\pi/4] , \tag{6}$$

$$\phi(R)=\int_a^R k(R)dR \ , \quad k(R)=\left[\frac{2m}{\hbar^2}(E-V(R))\right]^{1/2} , \tag{7}$$

where V are diabatic potentials, W_1 with bound states χ_v, W_2 with continuum states χ_c. For bound states $C_v=[2m\omega_v/\pi\hbar]^{1/2}$, and for continuum states $C_c=[2m/\pi\hbar^2]^{1/2}$; m is the reduced mass of the diatom and ω_v is the local (at v) vibrational frequency. Reexpressing the functions (6) as exponentials and applying the stationary-phase approximation, one obtains the stationary-phase condition for the phase difference $\Delta\phi(R)=\phi_2(R)-\phi_1(R)$,

$$\frac{d\Delta\phi}{dR}=k_2(R)-k_1(R) . \tag{8}$$

This defines the crossing point R_c when $E_v=E_c$, i.e., $W_1(R_c)=W_2(R_c)$. Expanding next the phase difference $\Delta\phi$ to second order about R_c and performing the Gaussian integral (5) gives for the diabatic photodissociation linewidth of the initial diabatic level v,

$$\Gamma_{v_d}=\frac{4\pi\omega_v}{v_c\Delta F_c}[V_{gu}(R_c)]^2\sin^2[\Delta\phi(R_c)+\pi/4] , \tag{9}$$

where v_c is the particle velocity at the crossing point R_c, ΔF_c is the difference in slope between the diabatic potentials, $\Delta F_c=|dW_1/dR-dW_2/dR|_{R_c}$, and $\Delta\phi(R_c)$ is now a composite phase integral,

$$\Delta\phi(R_c) = -\int_{a_1}^{R_c} k_1 dR + \int_{a_2}^{R_c} k_2 dR = \int_{a_2}^{R_c} k_2 dR + \int_{R_c}^{b_1} k_1 dR \ . \quad (10)$$

In obtaining (10) one uses the semiclassical quantization condition $\int_{a_1}^{b_1} k_1 dR = (v_d + 1/2)\pi$, where a_1 (b_1) is the left (right) turning point of the diabatic bound-state potential $W_1(R)$ and a_2 is the turning point of the dissociative potential $W_2(R)$. We see in Eq. (10) the appearance of a new phase and hence new bound state $\chi_+(R)$ *trapped* in the potential $W_+(R) = W_2(R)$ for $a_2 \geq R \geq R_c$ and $W_1(R)$ for $R_c \geq R \geq b_1$. We furthermore see that the diabatic photodissociation width Γ_{v_d} or photodissociation rate is zero when $\Delta\phi(R_c) + \pi/4 = m\pi$ where m is some integer. This stability of a diabatic resonance, and hence suppression of photodissociation, i.e., $\Gamma_{v_d} = 0$, occurs at such phase integral conditions.

We now turn to the strong-radiative-interaction case or *adiabatic* limit where now a significant avoided crossing (Fig. 1) is to be expected. Thus the new trapped state $\chi_+(R)$ discussed above with phase $\Delta\phi(R_c)$, Eq. (10), will evolve into a true adiabatic state of the laser-induced adiabatic potential, $W_+(R)$, Eq. (3), with frequency ω_+ and phase or action

$$\phi_+(R) = \int_{a_+}^{b_+} k_+ dR = (v_+ + \tfrac{1}{2})\pi \ , \qquad k_+ = \left[\frac{2m}{\hbar^2}(E - W_+(R)) \right]^{1/2} . \quad (11)$$

a_+ (b_+) are now the left (right) turning points of the adiabatic level v_+ on $W_+(R)$. The adiabatic state or function $\chi_+(R)$ is nonadiabatically coupled to the lower potential, $W_-(R)$, state $\chi_-(R)$. The adiabatic Fermi golden-rule expression for the widths Γ_{v_+} becomes now

$$\Gamma_{v_+} = 2\pi |\langle \chi_+(R) | V_{+-} | \chi_-(R) \rangle|^2 \ , \quad (12)$$

where

$$V_{+-}(R) = -\frac{\hbar^2}{2m} \frac{d\theta}{dR} \frac{d}{dR} \ , \quad (13)$$

$$\theta = \tfrac{1}{2} \tan^{-1} \{ 2V_{gu}(R) / [W_1(R) - W_2(R)] \} \ , \quad (14)$$

and θ is the nonadiabatic mixing angle [17,23,33].

Introducing the semiclassical approximations (6) for the adiabatic nuclear functions $\chi_\pm(R)$, one obtains after linearization of the diabatic potentials, V_{gu}, W_1, and W_2 in θ, and integrating at the crossing point R_c [16,23], the laser-induced resonance widths in the adiabatic (strong-radiative-coupling) limit,

$$\Gamma_{v_+} = \frac{\pi}{4} \hbar\omega_+ \exp \left[\frac{-\pi V_{gu}^2(R_c)}{\hbar \nu_c \Delta F_c} \right] \cos^2\beta \ , \quad (15)$$

$$\beta = \int_{a_-}^{R_c} k_- dR + \int_{R_c}^{b_+} k_+ dR \ . \quad (16)$$

ν_c and ΔF_c have been defined in Eq. (9). a_- and b_+ are the left and right turning points at energy E in the adiabatic potentials $W_{-(+)}(R)$ and ω_+ is the vibrational adiabatic frequency. The width of the adiabatic resonance, Eq. (15), is now a function of the phase integral β which defines a new state nearly equal to the original adiabatic state. The exponential factor is the Landau-Zener transition probability of nonadiabatic transitions [14–16].

In summary, photodissociation widths Γ_{v_d} or rates of diabatic (weak-field) states, Eq. (9), increase linearly with intensity I through $[V_{gu}(R_c)]^2$ but are further strongly dependent on an adiabatic phase factor, $\Delta\phi(R_c)$, Eq. (10). Adiabatic (strong-field) photodissociation widths Γ_{v_+}, Eq. (15), decreases exponentially with increasing intensity and furthermore vanish whenever there is *coincidence* (quasidegeneracy) of adiabatic and diabatic states, i.e., for values $\beta = (v + \frac{1}{2})\pi$, where v is the diabatic vibrational quantum number. Semiclassical solutions of the two coupled differential equations describing the time-independent Schrödinger equation for the two-potential system, Eq. (3) and Fig. 1, leads to the following general rule [14–16,23] : stability of laser-induced resonances or suppression of photodissociation occurs whenever diabatic states are coincident or quasidegenerate with adiabatic states. Further stabilization occurs at high intensities through the exponential Landau-Zener probability in Eq. (15) which decreases with increasing intensity.

The above analysis applies to the rotating-wave approximation, i.e., the two-state dressed representation illustrated in Fig. 1. Such an approximation is valid for electronic Rabi frequencies less than the excitation or photon frequency. In the present case, $\lambda = 212.8$ nm which gives a crossing point $R_c = 3$ a.u. (Fig. 1). Thus at an intensity of 10^{13} W/cm^2, one obtains from Eq. (2) $\omega_R \simeq 5000$ cm$^{-1} \simeq 0.6$ eV, whereas the corresponding photon energy ~ 6 eV. Hence, at $I = 10^{13}$ W/cm^2, we obtain $\omega_R / \omega_{\rm ph} \simeq 0.1$ whereas at $I = 10^{15}$ W/cm^2, $\omega_R / \omega_{\rm ph} \simeq 1$. One can therefore expect RWA and hence Fig. 1 to be applicable up to about 10^{13} W/cm^2. This is confirmed by our previous time-independent and time-dependent calculations which showed that RWA gave very similar results as the exact treatment at intensities below 10^{14} W/cm^2 [22]. This allows us therefore to correlate two-state time-independent calculations with the full time-dependent calculations in Sec. IV.

III. METHOD

A. Time independent

Time-independent stationary states of the field-molecule system were obtained by solving a two-state coupled equations system in the diabatic representation, i.e., with the potential matrix given in Eq. (3). The divergent radiative coupling, $\mu(R) = eR/2$, which is due to charge-resonance transitions [35], was truncated smoothly at 20 Å, thus ensuring stable results. The coupled equations were solved by a finite difference method, and integrated from $R = 0$, where the nuclear functions are zero, outward past 20 Å. Asymptotic analysis of the nuclear wave function gives an energy-dependent S matrix, which in turn gives the position E_r (Fig. 2) of the laser-

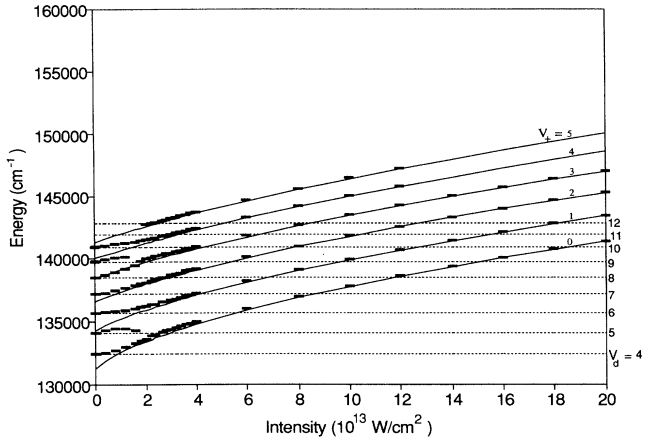

FIG. 2. Diabatic v_d (dotted lines) and adiabatic v_+ (solid lines) levels, and laser-induced resonance energies E_r(cm^{-1}) (horizontal bars) obtained from an S-matrix pole calculation for the two channels in Fig. 1.

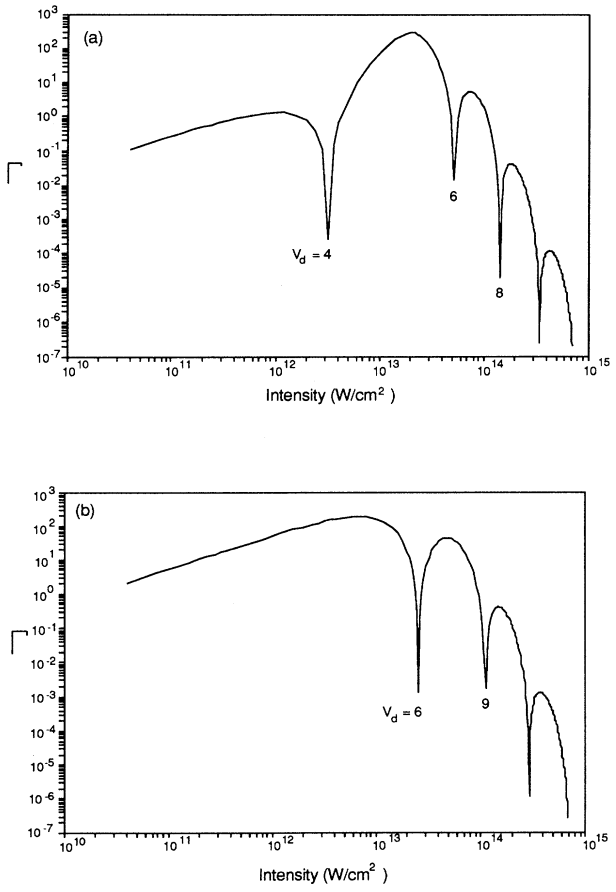

FIG. 3. Widths Γ_r(cm^{-1}) of laser-induced resonances converging to adiabatic levels (a) $v_{ad}=0$ and (b) 1. Corresponding energies are shown in Fig. 2 (horizontal bars). Minima occur at crossings of diabatic levels v_d with the adiabatic levels $v_+ \equiv v_{ad}$ (Fig. 2).

induced resonances and their widths Γ_r (Fig. 3) [15,17–20].

B. Time dependent

For the rotationless calculations the time-dependent Schrödinger equation for the nuclear states $\chi_g(R,t)$ and $\chi_u(R,t)$, $\chi=[\chi_g,\chi_u]$,

$$\left[i\hbar\frac{\partial}{\partial t}+\frac{\hbar^2\nabla^2}{2m}\right]\chi(R,t) = \begin{bmatrix} V_g(R)-\mu_a V_{gu} & V_{gu}(R,t) \\ V_{gu}(R,t) & V_u(R)-\mu_a V_{gu} \end{bmatrix}\chi(R,t)\ , \quad (17)$$

is solved using the second-order split-operator method, where the exponential of the Laplacian is evaluated using the fast-Fourier-transform method [36–38]. The potentials $V_g(R)$ and $V_u(R)$ are the unperturbed potentials of H_2^+, $V_{gu}(R,t)=(eR/2)E_0(t)\cos\omega t$, where $R/2$ is the electronic transition moment $\langle 1\sigma_g|r|2p\sigma_u\rangle$ [35]. $E_0(t)$ is the pulse envelope taken to be a constant amplitude of 98 fs with a 1 fs rise and fall of the field. The diagonal permanent transition moment μ_a was applied for HD^+ only, and is defined as $\mu_a=(m_D-m_H)/(m_D+m_H)$ [39]. Such a permanent dipole moment occurs for noncentrosymmetric systems, and gives rise to important isotope effects in high (static) field dissociation.

For calculations including rotation, the nuclear wave function is expanded into rotational basis functions, $\chi=[\chi_J]$, where J is the total angular-momentum quantum number. Electronic transitions where $\Delta J=0$ were neglected, hence only $\Delta J=\pm1$ transitions were retained. This is reasonable because the coupling constant V_{JJ} is much smaller than V_{JJ+1} for $J>0$ [40], and all calculations were performed for initial $J=5.5$. The potential matrix has diagonal elements $V_i(R)+\hbar^2N_i(N_i+1)/(2\mu R^2)$, where $i=1,2$, $V_1=V_g$, $V_2=V_u$, and $N_i=2k-i(k=1,2,3,\ldots)$, and off-diagonal elements $V_{JJ+1}=V_{gu}[(J+1+m_J)(J+1-m_J)]^{1/2}/2(J+1)$. Separate calculations were done for each positive m_J sublevel. It should be pointed out that even though single ionization of H_2 at high fields will produce H_2^+ in states with high J and low m_J, scattering of H_2^+ with the ionized electron

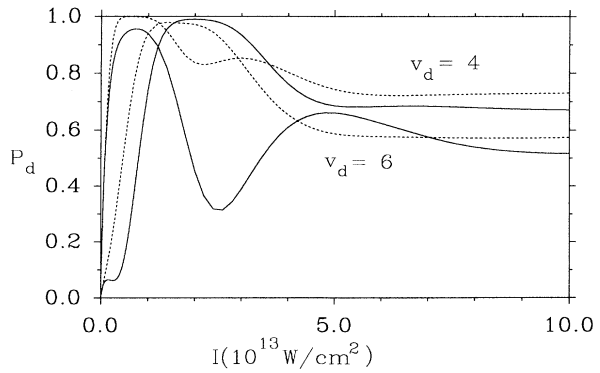

FIG. 4. Photodissociation probability for initial levels $v_d=4$, 6 for H_2^+ (solid lines) and HD^+ (dashed lines), 100-fs pulses at $\lambda=212.8$ nm.

will randomize the m_J's. We will show that alignment of H_2^+, which occurs with high J and low m_J, can result from rotational pumping of H_2^+, and therefore does not rely on the effect of ionization of H_2.

Taking as initial condition $\chi_v(R,t=0)$ [or $\chi_{5.5,m_J}(R,t=0)$], one propagates in time [Eq. (17)] the nuclear wavefunction χ_v (or χ_{J_i,m_j}) discretized in space, allowing us to obtain the ground $\chi_g(R,t)$ [or $\chi_{J_1,m_J}(R,t)$] and excited $\chi_u(R,t)$ [or $\chi_{J_2,m_J}(R,t)$] nuclear functions until they propagate freely on the diabatic (unperturbed) potentials $V_g(R)$ and $V_u(R)$ after the end of the pulse. The time step was taken to be 1/100 of the period of the laser, and the space grid division was chosen small enough to ensure that the Fourier transform of the wave function was bandwidth limited. Enough rotational levels were used to obtain converged results, a number which varied form 9 to 35 for intensities 10^{12} and 10^{14} W/cm^2, respectively. After the pulse is over one can integrate the density $|\chi_u(R,t)|^2$ (or $|\chi_{J_2,m_J}|^2$) from a point R_d outside the right turning point of the upper $W_+(R)$ surface ($R_d \geq 3$ Å) to obtain the dissociation probabilities P_d (Fig. 4). We note that, in general, one should integrate the total nuclear wave function to obtain P_d, because of the possibility of absorbing an even number of photons leading to dissociation into the ground electronic state. However, under our conditions only single-photon absorption was observed, and thus dissociation was obtained only in the excited electronic state.

The angular distribution of products (for initial $J=5.5$) is

$$P_d(\theta)=\frac{1}{11}\sum_{m_N=0}^{5} W_m \sum_{\Omega=-1/2}^{1/2} \int_{R_d}^{\infty} dR \left| \sum_{\substack{N=m_N \\ (N \text{ even})}}^{N_{\max}} \chi_{J,m_J} \left[\frac{2J+1}{4} \right]^{1/2} d^J_{m_J,\Omega}(\theta) \right|^2 , \tag{18}$$

where $d^J_{m_J,\Omega}(\theta)$ is the rotation matrix [41], $J=N+\frac{1}{2}$, $m_J=m_N+\frac{1}{2}$, $W_m=2$ for $m_N>0$ and $W_m=1$ for $m_N=0$.

IV. RESULTS

A. Time independent

Resonance energies E_r are shown in Fig. 2, along with the diabatic $E(v_d)$ (field-free) and adiabatic $E(v_+)$ levels [obtained from adiabatic potentials $W_+(R)$]. Both $E(v_d)$ and $E(v_+)$ are obtained as resonances in a S-matrix two-channel calculation involving an arbitrary continuum channel coupled to the molecular potentials W or W_+. In the low-intensity limit the resonances energies are equal to the diabatic (unperturbed) energies. As the intensity increases, *resonance locking* occurs. For example, the $v_d=4$ level converges to the adiabatic $v_+=0$ level. Such locking occurs only for diabatic levels which are slightly above an adiabatic level at low intensity. The $v=5$ and $v=9$ levels, which are slightly below an adiabatic level at low intensity, do not converge initially to any adiabatic level. At higher intensity they eventually stabilize due to the Landau-Zener effect, Eq. (15). Also, time-dependent calculation of photodissociation from $v=5$ [22] yields no minimum in P_d vs I, unlike results for $v=4$ and $v=6$ (see the next section). Figure 3 shows the linewidths Γ_r for resonances converging to $v_{\text{ad}} \equiv v_+ = 0$ and 1. Sharp minima in Γ_r occur at those intensities where a diabatic level crosses an adiabatic level in Fig. 2. This confirms the stabilization rule given in Sec. II. Three minima relevant to our time-independent results, and shown in Fig. 3, occur at coincidences of $v_d=4$ and $v_+=0$ (3.2×10^{12} W/cm^2), and of $v_d=6$ and $v_+=0,1$ (5.2×10^{13}, 2.6×10^{13} W/cm^2).

A further stabilization is evident in Fig. 3 as the resonance linewidth decreases with increasing intensity. This is consistent with the decrease of the linewidth Γ_{v_+} with increasing intensity, Eq. (15), due to the exponential dependence on intensity. At high intensity, $I>10^{14}$ W/cm^2, $\Gamma_{v_+}<10^{-4}$ cm^{-1}, implying that the adiabatic limit has been reached, and the energy of the laser-induced resonance is that of the adiabatic level. This is clearly illustrated in Fig. 2, as all resonances converge to some adiabatic level v_+.

B. Time dependent

Figure 4 shows an initial increase of the dissociation probability for the initial vibrational levels $v_d=4,6$, for H_2^+ and HD^+. With increasing intensity saturation occurs, followed by minima (for H_2^+) at 3.2×10^{12} W/cm^2 for $v_d=4$, and 2.6×10^{13} W/cm^2 for $v_d=6$. These minima correspond precisely to minima in the linewidths of $v_+=0,1$ (Fig. 3). In all curves in Fig. 4, a constant plateau is reached at intensities above 5×10^{13} W/cm^2, and persists at intensities at which the adiabatic minimum is above the initial diabatic level [22]. Examination of the kinetic-energy distribution of products (Fig. 6 in [22]) reveals sharp peaks at high energies, resulting from nonadiabatic transitions from the initial diabatic level to more highly excited levels.

For HD^+, which now has a permanent dipole moment μ_a, photodissociation from $v_d=4$ leads to marginal stabilization around 2×10^{13} W/cm^2, while dissociation from $v_d=6$ is not stabilized at all, except at high intensities (as is the case for photodissociation from all initial levels of H_2^+ and HD^+). The isotope effect is most striking for $v_d=4$ at 3×10^{12} W/cm^2, where 10% of H_2^+ versus 100% of HD^+ dissociates. Note that at low intensity the Fermi golden rule applies, so that the curves for $v_d=4$ of HD^+ and $v_d=6$ of H_2^+ have the same linear behavior. Note also that the curves for $v_d=6$ of HD^+

and $v_d=4$ of H_2^+ have the same initial gradient, although the former does not exhibit a minimum. The difference between the results for H_2^+ and HD^+ is a consequence solely of the difference in reduced mass, which leads to diabatic-adiabatic coincidences at different intensities for different initial levels (the crossing point is 0.02 eV below $v_d=2$ for H_2^+ and 0.06 eV above $v_d=2$ for HD^+). It was found that the diagonal transition moments μ_a of HD^+ have no influence on the results. This is not surprising, since the laser frequency oscillates too fast (8.85 fs^{-1}) compared to the vibrational spacings (~ 0.3 fs^{-1}) to cause any purely vibrational transitions. Thus the isotope effect is solely due to different coincidences of adiabatic and diabatic levels in H_2^+ and HD^+.

The influence of rotational excitation has been addressed previously in Refs. [40,42] in a time-independent (dressed-state) framework. In the present time-dependent simulation multiple rotational excitation at intensities of 10^{14} W/cm^2 resulted in no stabilization at all. At lower intensities, stabilization is observed for initial level $v_d=4$, $J=5.5$, $m_J=0.5$ at 9×10^{12} W/cm^2 ($P_d=0.31$), and for $v_d=6$, $J=5.5$, $m_J=0.5$ at 3×10^{13} W/cm^2 ($P_d=0.89$), denoted by dotted lines (squares) in Fig. 5. We extend the above results to include all rotational m_J sublevels, and the effect of stabilization of the $m_J=0.5$ sublevel (where the molecule is parallel to the field polarization) on the angular distribution of products. All of the results are for the initial rotational level $J=5.5$.

At high intensities, significant rotational excitation can lead to products with values of J much larger than m_J, which results in the molecule tending to align itself with the field (note that linear polarization is used, hence $\Delta m_J=0$). However, if one chooses an intensity where the $m_J=0.5$ component is stabilized with respect to the other sublevels, then one will obtain an angular distribution which is peaked at higher angles [40]. Angular distributions for selected intensities and initial levels are shown in Fig. 6. The solid curve in Fig. 6(a), for $v_d=4$ at 5×10^{12} W/cm^2, shows a typical result at low intensity: the distribution is fairly diffuse with a maximum around 40 ° with respect to the laser polarization. The same shape is obtained at the same intensity for $v_d=6$, where the dissociation probability is near a maximum for $m_J=0.5$ (see Fig. 5). The dashed curve in Fig. 6(a), for $v_d=4$ at 9×10^{12} W/cm^2, shows the effect of mild stabilization of the $m_J=0.5$ sublevel of $v_d=4$: the distribution is shifted slightly to higher angles, as in previous time-independent calculations [40,42].

A more significant effect of stabilization on angular distribution is shown in Fig. 6(b). The solid curve, $v_d=4$ at 3×10^{13} W/cm^2, shows a typical distribution at high intensity: a more strongly peaked distribution than at lower intensity, and a maximum around 30 °. A distribution of the same shape was obtained for $v_d=4$ at 10^{14} W/cm^2. At 3×10^{13} W/cm^2, the dissociation probability for $v_d=6$, $m_J=0.5$ is at a minimum. This results in an angular distribution for $v_d=6$ with a peak at 10 °, and a higher peak at 55 ° [dashed curve in Fig. 6(b)].

The shift of the angular distribution to higher angles always occurs when photodissociation from the $m_J=0.5$ sublevel is at a minimum. Since increasing m_J is equivalent to decreasing the intensity [40], i.e., weaker radiative coupling, the other sublevels will be destabilized with respect to the $m_J=0.5$ sublevel, and the products appear at higher angles. Such disalignment of a molecule undergoing a Σ_g-Σ_u transition at high intensity has previously been predicted from time-independent coupled-equation calculations for Ar_2^+ [40,42]. Our time-dependent results show that even for short pulses (100 fs),

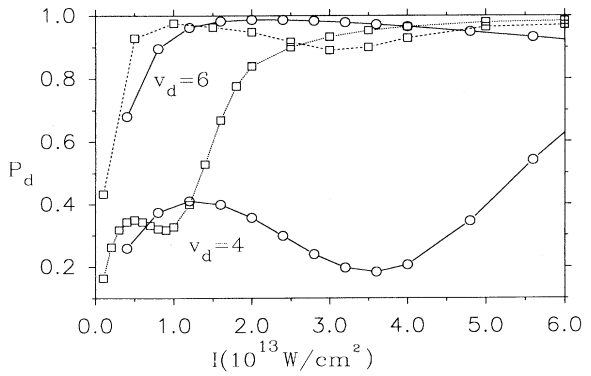

FIG. 5. Photodissociation probability for initial sublevels $J=5.5$, $m_J=0.5$ of $v_d=4$ and 6, obtained by full rotational (dashed line) and two potential (Σ_g, $J=5.5$, and Σ_u, $J=6.5$; solid lines) calculations. $\Delta m_J=0$.

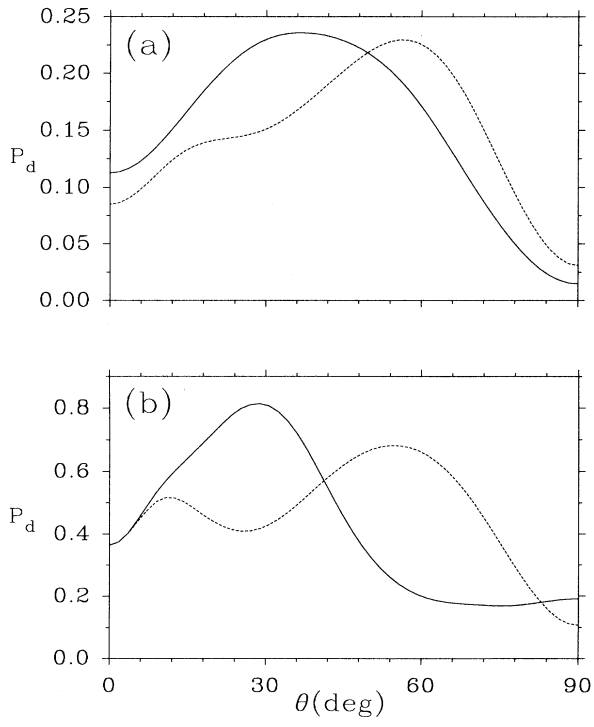

FIG. 6. Angular distribution of photodissociation products [Eq. (18)] for initial $J=5.5$. (a) $v_d=4$, $I(\mathrm{W/cm^2})=5\times10^{12}$ (solid line) and 9×10^{12} (dashed line). (b) $I(\mathrm{W/cm^2})=3\times10^{13}$, $v_d=4$ (solid line) and 6 (dashed line). $\Delta m_J=0$.

of the same order as the rotational period (91 fs for $J=5.5$ at $R=1$ Å), significant rotational excitation can occur, leading to alignment or disalignment with the laser polarization.

V. DISCUSSION

The present results establish laser-induced avoided crossings as an important source for stabilization of laser-induced resonances and hence for suppression of dissociation at high intensities. Two mechanisms are operative and are summarized by linewidth expressions (9) and (15). First, coincidence or quasidegeneracy of diabatic (zero-field) and adiabatic (field-induced) vibrational levels results in stable resonances (see Figs. 2–3). This translates into minima in the photodissociation probabilities for short-pulse excitation (Fig. 4). Second, with increasing intensity, *trapping* of the initial state into stable adiabatic states occurs due to the decoupling of these states at high intensities, i.e., in the adiabatic regime nonadiabatic couplings [Eq. (14)] diminish with increasing radiative interaction, or equivalently, with increasing gaps between the adiabatic potentials $W_{\pm}(R)$ (Fig. 1) [14–17,22]. This effect can be explicitly seen in the adiabatic limit photodissociation width Γ_{v_+}, Eq. (15). The Landau-Zener–type expression shows that adiabatic widths behave as $\exp(-\alpha I)$ at high intensities. This is corroborated by the envelope of the widths as a function of I illustrated in Fig. 3. Initially one has the linear diabatic regime increase with intensity, Eq. (9), and finally the exponential decrease, Eq. (15). The minima, corresponding to total suppression of dissociation are of course the signature of the coincidences of diabatic and adiabatic levels due to the dependence of the widths on the adiabatic or diabatic phases or actions. Similar stabilization related to trapping has also been found from simulations with Gaussian pulses [30–32]. However, in such cases no correlation with the dressed (time-independent) states has been performed. We emphasize that using nearly square pulses as in the present case, stabilization is directly related to crossings of diabatic and adiabatic states as discussed in the previous section.

The effect of rotational excitation, which can go as high as $\Delta J=35$ at 10^{14} W/cm^2, has been recognized in previous time-independent calculations [40,42] to stabilize or destabilize laser-induced resonances. Thus diabatic and adiabatic levels which are coincident in a two-channel calculation [solid lines (circles) in Fig. 5] become destabilized upon rotational excitation. The stability intensity will therefore move to lower intensities since multiple excitations to the dissociative (continuum) channels corresponds to larger effective radiative coupling. This is clearly seen for the $v_d=4$ level in Fig. 5 where the two-channel stability intensity decreases from 3.5 to 1×10^{13} W/cm^2 upon rotational excitation of the $m_J=\frac{1}{2}$ component of the initial $J=5.5$ level. Conversely, diabatic and adiabatic levels which are nondegenerate in a two-channel calculation, hence implying unstable and therefore rapidly dissociating resonances, can be made coincident by rotational excitation, and thus become more stable (e.g., $v_d=6$ level in Fig. 5). However, this is not a very efficient stabilization mechanism at high intensities, where rotationally induced coincidence and multiple continuum excitations compete against each other.

The angular distributions illustrated in Fig. 6 demonstrate the influence of the different dissociation probabilities of each m_J component of an initial J level. At the stability points of the smallest $m_J=\frac{1}{2}$, Fig. 5, the molecule which is in a parallel orientation ($\theta=0$) with respect to the field is dissociating slower than other m_J components which correspond to orientations away from the parallel one ($\theta>0$). In the weak-field, perturbative limit, one expects a $\cos^2\theta$ distribution for a $\Sigma\rightarrow\Sigma$ transition [41]. Figure 6 shows a peaking of angular distributions at smaller angles for unstable or rapidly dissociating $m_J=\frac{1}{2}$ components and bimodal (two maxima) for stable or slowly dissociating $m_J=\frac{1}{2}$ components. In the first case, the other m_J components also contribute significantly at other angles, thus creating a peak at an angle $\theta\neq0$. In the last case of a stable $m_J=\frac{1}{2}$ component ($\theta=0$), the larger m_J components are dissociating more rapidly than the small m_J components, thus causing the bimodal distribution as seen in Fig. 6.

The successful correlation obtained between the two-channel dressed-state time-independent representation (Figs. 1–3) and the exact time-dependent results (Figs. 4–6) depend on the applicability of the rotating-wave approximation up to intensities of about 10^{13} W/cm^2 as discussed at the end of Sec. II. Deviations occur from this representation at $I=10^{14}$ W/cm^2. Thus Eq. (15) and Fig. 3 predict decreasing dissociation with increasing intensity, whereas Fig. 4 points to a plateau of around 60% dissociation at $I=10^{14}$ W/cm^2. This is indicative of the contribution of higher-order dressed states, $\Delta n>\pm1$, due to virtual transitions whenever the Rabi frequency ω_R, Eq. (2), approaches the photon frequency [18–20]. Furthermore at such high intensities, the electronic Rabi frequency for the $\Sigma_g\rightarrow\Sigma_u$ transition approaches the frequency of higher excitation. In particular, recent calculations for H_2^+ show that ionization rates approach 10^{13}–10^{14} s^{-1} at $I=10^{14}$ W/cm^2 [43]. We conclude therefore that rotational excitations and ionization preclude any stabilization of molecular ions above 10^{13} W/cm^2 for subpicosecond excitation. The conclusion seems to be in agreement with recent experiments on multiphoton ionization of other molecular species such as I_2 and HCl [44,45].

ACKNOWLEDGMENTS

We thank the Natural Sciences and Engineering Research Council of Canada for financing this research through operating grants and through the National Center of Excellence in Molecular Dynamics.

[1] M. H. Mittleman, *Introduction to the Theory of Laser-Atom Interactions* (Plenum, New York 1982).
[2] *Atomic and Molecular Processes with Short Intense Laser Pulses,* Vol. 171 of *NATO ASI, Series B: Physics,* edited by A. D. Bandrauk (Plenum, New York, 1988).
[3] J. van de Ree and J. Z. Kaminski, Phys. Rev. A **37** 4536 (1988).
[4] M. Fedorov and J. Movsesian, J. Opt. Soc. Am. B **6**, 928 (1989).
[5] Q. Su, J. H. Eberly, and J. Javanainan, Phys. Rev. Lett. **64**, 862 (1990).
[6] J. Parker and C. R. Stroud, Phys. Rev. A **41**, 1602 (1990).
[7] Y. Dubrovskii, M. Ivanov, and M. Fedorov, Zh. Eksp. Teor. Fiz. **99**, 411 (1991) [Sov. Phys. JETP **72**, 228 (1991)].
[8] *Coherent Phenomena in Atoms and Molecules in Laser Fields,* Vol. 287 of *NATO ASI, Series B: Physics,* edited by A. D. Bandrauk and S. C. Wallace (Plenum, New York, 1992).
[9] C. Cohen-Tannoudji and S. Reynaud, in *Multiphoton Processes,* edited by J. H. Eberly and P. Lambropoulos (Wiley, New York, 1983).
[10] N. M. Kroll and K. M. Watson, Phys. Rev. A **13**, 1018 (1976).
[11] A. I. Voronin and A. A. Samokhin, Zh. Eksp. Teor. Fiz. **70**, 9 (1976) [Sov. Phys. JETP **43**, 4 (1976)].
[12] A. M. Lau and C. K. Rhodes, Phys. Rev. A **16**, 2392 (1977).
[13] J. M. Yuan and T. F. George, J. Chem. Phys. **68**, 3040 (1978).
[14] A. D. Bandrauk and M. L. Sink, Chem. Phys. Lett. **57**, 569 (1978).
[15] A. D. Bandrauk and M. L. Sink, J. Chem. Phys. **74**, 1110 (1981).
[16] A. D. Bandrauk and J. F. McCann, Comments At. Mol. Phys. **22**, 325 (1989).
[17] T. T. Nguyen-Dang and S. Manoli, Phys. Rev. A **44**, 5841 (1991).
[18] A. D. Bandrauk and J. M. Gauthier, J. Opt. Soc. Am. B **7**, 1420 (1990).
[19] A. Giusti-Suzor, X. He, O. Atabek, and F. H. Mies, Phys. Rev. Lett. **64**, 515 (1990).
[20] A. D. Bandrauk, E. Constant, and J. M. Gauthier, J. Phys. (France) II **1**, 1033 (1991).
[21] A. D. Bandrauk, E. E. Aubanel, and J. M. Gauthier, Laser Phys. **3**, 381 (1993).
[22] E. E. Aubanel, A. D. Bandrauk, and P. Rancourt, Chem. Phys. Lett. **197**, 419 (1992).
[23] A. D. Bandrauk and M. S. Child, Mol. Phys. **19**, 95 (1970).
[24] J. W. J. Verschuur, L. D. Noordam, and H. B. van Linden van den Heuvell, Phys. Rev. A **40**, 4383 (1989).
[25] P. H. Bucksbaum, A. Zavriyev, H. G. Muller, and D. W. Schumacher, Phys. Rev. Lett. **64**, 1883 (1990).
[26] P. H. Bucksbaum, A. Zavriyev, H. G. Muller, and D. W. Schumacher, Phys. Rev. A **42**, 5500 (1990).
[27] S. W. Allendorf and A. Szoke, Phys. Rev. A **44**, 518 (1991).
[28] H. Helm, M. J. Dyer, and H. Bissantz, Phys. Rev. Lett. **67**, 1234 (1991).
[29] A. Zavriyev, P. H. Bucksbaum, J. Squier, and F. Salin, Phys. Rev. Lett. **70**, 1077 (1993).
[30] A. Giusti-Suzor and F. H. Mies, Phys. Rev. Lett. **68**, 3869 (1992).
[31] G. Yao and S. I. Chu, Chem. Phys. Lett. **197**, 413 (1992).
[32] G. Jolicard and O. Atabek, Phys. Rev. A **46**, 5845 (1992).
[33] H. Lefebvre-Brion and R. W. Field, *Perturbations in Spectra of Diatomic Molecules* (Academic, Orlando, FL, 1986).
[34] M. S. Child, *Molecular Collision Theory* (Academic, London, 1974).
[35] R. S. Mulliken, J. Chem. Phys. **7**, 20 (1939).
[36] R. Heather and H. Metiu, J. Chem. Phys. **86**, 5009 (1987).
[37] A. D. Bandrauk and H. Shen, Chem. Phys. Lett. **176**, 428 (1991); Can. J. Chem. **70**, 555 (1992).
[38] M. D. Feit and J. A. Fleck, J. Chem. Phys. **78**, 2578 (1984).
[39] J. R. Hiskes, Phys. Rev. **122**, 1207 (1961).
[40] A. D. Bandrauk and G. Turcotte, J. Chem. Phys. **77**, 3867 (1982); J. Phys. Chem. **87**, 5098 (1983).
[41] R. N. Zare, *Angular Momentum* (Wiley, New York, 1988).
[42] J. F. McCann and A. D. Bandrauk, Phys. Rev. A **42**, 2806 (1990); J. Chem. Phys. **96**, 903 (1992).
[43] S. Chelkowski, T. Zuo, and A. D. Bandrauk, Phys. Rev. A **46**, 5342 (1992).
[44] D. T. Strickland, Y. Beaudoin, P. Dietrich, and P. B. Corkum, Phys. Rev. Lett. **68**, 2755 (1992).
[45] P. Dietrich and P. B. Corkum, J. Chem. Phys. **97**, 3187 (1992).